Numerical and experimental investigation of sound transmission through roller shutter boxes

Soraya Bakhouche, Walid Larbi, Jean-François Deü, Philippe Macquart

Available online at www.sciencedirect.com

SciVerse ScienceDirect

Applied Acoustics 00 (2023) 000–000

Numerical and experimental investigation of sound transmission through roller shutter boxes

Soraya Bakhouche[a], Walid Larbi[a]*, Jean-François Deü[a], Philippe Macquart[b]

[a]*Conservatoire national des arts et métiers (Cnam), Laboratoire de Mécanique des Structures et des Systèmes Couplés (LMSSC), 2 rue Conté, 75003 Paris, France*

[b]*Union des Fabricants de Menuiseries (UFME), 39 rue Louis Blanc, 92038 Courbevoie, France*

Abstract

Roller shutter boxes are essential components of building facades, providing crucial thermal and acoustic insulation. Conventional laboratory tests have been traditionally used to evaluate the sound transmission of roller shutter boxes. However, these tests can be expensive and lack repeatability and reproducibility, especially in the low-frequency range. To overcome these limitations, this study aims to introduce an advanced numerical model capable of accurately predicting the vibroacoustic response of roller shutter boxes and optimizing their acoustic insulation performance. The proposed numerical approach utilizes the finite element method to model the various solid and fluid domains within the roller shutter box structure. To capture the behavior of the poroelastic layers, a mixed displacement-pressure formulation of the Biot poroelasticity equations is employed. Excitation of the structure is achieved using a diffuse field comprising a superposition of plane waves with random phases and directions, while the resulting sound radiation is computed utilizing the infinite elements method. To validate the proposed numerical model, a comparison is made with results obtained from laboratory tests, and the experimental protocol is thoroughly described. The practical application of the proposed numerical method extends to the investigation of several influential factors on the acoustic behavior of roller shutter boxes, including assembly conditions, the positioning of poroelastic layers, and the inclusion of heavy masses.

Keywords: roller shutter box, experimental test, numerical simulation, porous material

1. Introduction

Effective acoustic performance in building facades is crucial to minimize disturbances within buildings. Building standards often define a minimum requirement for the apparent sound insulation of facades, which considers the contribution of various components, including windows, air inlets, and roller shutter boxes. However, these components often represent the weakest links in terms of acoustic insulation, making it essential to understand their individual acoustic performance to achieve facades with satisfactory sound insulation. The sound insulation of building elements is typically evaluated through sound transmission loss (TL) measurements using experimental tests based on established standards [1]. These tests are conducted in acoustic laboratories using two finite-sized rooms and one or more loudspeakers to generate sound field

*Corresponding author.

E-mail address: walid.larbi@lecnam.net (W. Larbi).

excitation. The tests assume negligible lateral transmission and a perfectly diffuse sound field, where the acoustic intensity is uniform at all points within the rooms. However, it is important to note that below the Schroeder frequency [2], a diffuse field condition cannot be assumed due to the dominance of a few modes in the rooms, especially at low frequencies. Numerous investigations have highlighted the significant dependence of experimental methodologies on room conditions, particularly at extremely low frequencies [3]. This indicates that transmission loss predictions are only applicable to the specific test scenario. Additionally, sound transmission loss results for the same sample have been found to vary between different test laboratories. To analyze the specific characteristics of each situation and overcome the limitations of traditional experimental tests, numerical approaches can be employed to provide more representative measurement conditions. Numerical methods, such as the Finite Element Method (FEM) [3,4,5], along with energetic methodologies like Statistical Energy Analysis (SEA) or Matrix Transfer Method (TMM), are available to address the sound insulation problem [6,7,8]. The choice of method depends on factors such as computing cost and the frequency range of interest. We can cite for example the work of Yang Y et al. in [4] where the authors introduced an extension of the wave and finite element (WFE) method for predicting sound transmission and radiation in infinite panels. It combines finite element analysis with analytical models of surrounding acoustic spaces, yielding efficient and accurate predictions. The method is successfully validated through numerical examples, demonstrating good agreement with analytical results. Computational times are minimized due to the small size of the WFE model. The same authors proposed in [5] a novel method for predicting vibroacoustic responses in periodic structures, combining wave and finite element analysis with space-harmonic assumptions. It successfully demonstrates the method's accuracy through numerical examples, validating its predictions against analytical and literature results. This efficient approach offers practical benefits for analyzing complex periodic structures. Note that numerical methods used for analyzing sound insulation properties of building components, such as finite element or boundary element methods, are typically more accurate in the lower frequency range. As frequencies increase, the wavelengths become smaller, and at higher frequencies, numerical methods might require finer meshing and more complex models, which can significantly increase computational time and resource requirements.

These numerical approaches offer greater flexibility and accuracy in analyzing the acoustic behavior of complex systems like roller shutter boxes. In this context, this study focuses specifically on the sound transmission loss of roller shutter boxes, which are essential components of building facades. These boxes are evaluated according to laboratory requirements. However, precise acoustic data replication has proven to be a significant challenge in these tests, as highlighted by these references [9, 10,11]. Additionally, the position of the curtain, whether extended or retracted, has a significant impact on the transmission loss. The choice of sound insulation material is also crucial, with the combination of melamine foam and heavy masses offering optimal insulation. To address these concerns and provide a reliable technique for predicting the acoustic behavior of both extended and retracted roller shutter boxes, this study combines numerical analysis and experimental data.

Limited research has been conducted on the acoustic evaluation of roller shutter boxes, and only a few accessible bibliographic references are available. Asdrubali and Buratti [12] tested different prototypes of high sound insulation ventilating windows with and without shutter boxes. Meanwhile, Diaz and Pedrero [13] reviewed research on sound insulation from airborne noise in various window types (such as double side-hung casement and double horizontal sliding sash) with built-on shutters and prefabricated boxes. The authors investigated the impact of the interior finish of the shutter box and the shutter position, whether fully retracted or extended, on each window type. To the authors' knowledge, there are no bibliographic references addressing the use of numerical techniques for the acoustic characterization of roller shutter boxes, which

makes this study original in its contribution. Moreover, within the same research framework, the authors have recently employed numerical prediction and experimental calibration methodologies to analyze the sound transmission properties of windows and double glazing [14]. This prior work enhances the expertise and methodology utilized in the present study on roller shutter boxes, contributing to a comprehensive understanding of the acoustic behavior of building components.

This work aims to investigate the sound transmission characteristics of roller shutter boxes and propose design improvements for better acoustic performance across a frequency range between 100 Hz and 1000 Hz. The impact of roller shutter boxes on facade sound insulation is most notable at higher frequencies. These frequencies tend to coincide with points of greater vulnerability, where air openings and potential leaks are more prominent. Although the experimental sound reduction index was measured across a range of 100 to 5000 Hz, we have chosen to focus the presentation in this article on frequencies up to 1000 Hz. This decision aligns with the limitations of the numerical method we employed, which primarily addresses the lower frequency spectrum. This approach allows for a more effective comparison between the experimental and numerical results.

The paper is structured as follows:

Section 2 provides a detailed description of the roller shutter box design, meticulously examining its construction and constituent components. This section highlights the key elements that have a significant influence on sound transmission.

In Section 3, the research focuses on conducting experimental measurements to assess the sound transmission loss of the roller shutter box set according to ISO 10140:2010 standards. Laboratory measurements and advanced acoustic techniques are employed to evaluate the effectiveness of these boxes in reducing sound transmission.

Section 4 explores the finite element formulation of the coupled elastoacoustic problem with poroelastic treatment for noise reduction. A mixed displacement-pressure formulation of the Biot poroelasticity equations is employed to model the poroelastic domain. The section presents the local equations and coupling conditions between different domains. Finite element discretization techniques are proposed for accurate numerical solutions. Additionally, the study incorporates modeling of diffuse field excitation and utilizes the Rayleigh integral and the Infinite Element Method for estimating the acoustic radiated power.

Section 5 concentrates specifically on sound transmission through the roller shutter box, employing the proposed numerical model in section 4 to simulate and analyze its acoustic behavior. This section provides a comprehensive description of the numerical configuration of the problem and establishes a correlation between the numerical results and the experimental findings, ensuring the reliability of the simulations.

In Section 6, a parametric analysis is conducted to thoroughly investigate the factors influencing sound transmission in the roller shutter box. The analysis encompasses critical parameters such as the presence of end caps, the boundary conditions, the positioning of sound insulation material, and the optimal placement of heavy masses.

2. Roller shutter box design description

A roller shutter box (Fig.1) is an enclosure typically installed above a window to house a roller shutter system. It provides a secure and compact storage space for the roller shutter when it is extended or retracted. The box is designed to protect and conceal the roller shutter mechanism when it is not in use. The elements included in a roller shutter box can vary depending on the specific design and manufacturer. However, here are the common components described as follows.

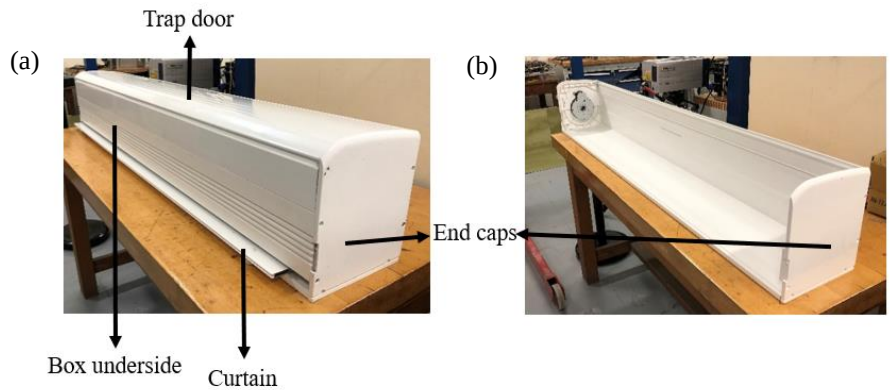

Fig. 1. (a) Retracted roller shutter box and (b) interior of the box without the curtain, the trapdoor and the box underside

The box casing is the main structure that surrounds and houses the roller shutter. It is usually made of aluminum or PVC and is available in different sizes to accommodate various shutter dimensions. The boxes are made of double-leaf panels with stiffeners for several reasons. This design helps to reduce the weight of the roller shutter box without compromising its strength. The stiffeners also distribute the load evenly across the box, making it more resistant to bending or deformation. These can also contribute to thermal insulation. The air trapped within the panel cells acts as a natural insulator, reducing heat transfer between the external and internal environments.

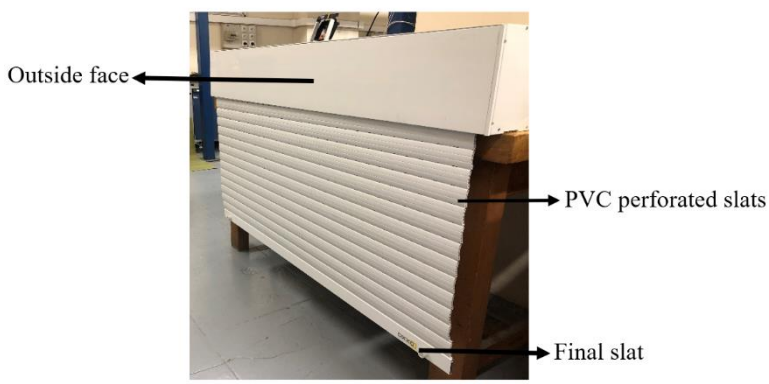

Fig. 2. Extended roller shutter box

The box also includes a trapdoor providing access to the interior of the box for maintenance, repairs, or adjustments. The end caps are fitted on both ends of the box casing to seal and secure the roller shutter inside. The end caps help maintain the overall integrity of the box and prevent dust, debris, or insects from entering. The guide rails are vertical tracks installed on the sides of the window frame. The roller shutter slides up and down within these tracks when operated. The guide rails ensure smooth and stable movement of the shutter.

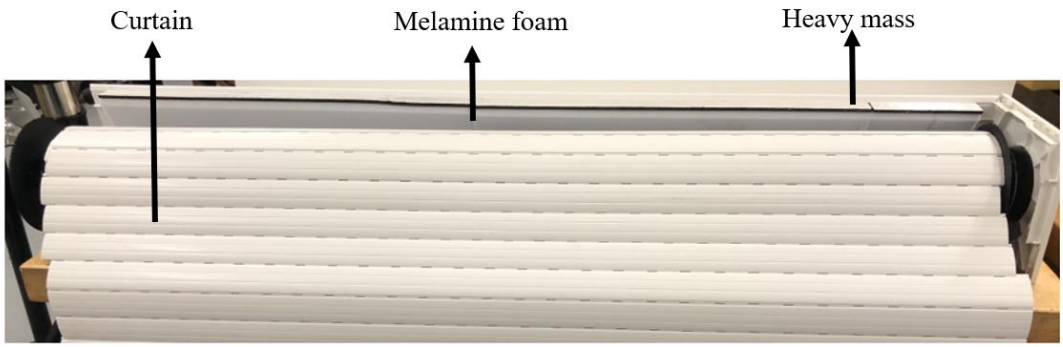

Fig. 3. Internal construction of the roller shutter box with insulation material

The shutter curtain (Fig.2 and Fig.3) is the movable part of the roller shutter that comprises individual slats or panels. These slats are usually made of aluminum or PVC and are interconnected to form a continuous curtain. The slats are designed to provide security, insulation, and protection against noise, sunlight, and weather conditions. Two groups of slats can be distinguished: full and hollow. The hollow slats can be filled with insulation materials such as polyurethane foam. The end slat, also known as the final slat or end plate, is a component of a roller shutter system that serves as the closing element at the bottom of the roller shutter curtain. It is specifically designed to provide a secure and tight seal when the roller shutter is fully closed.

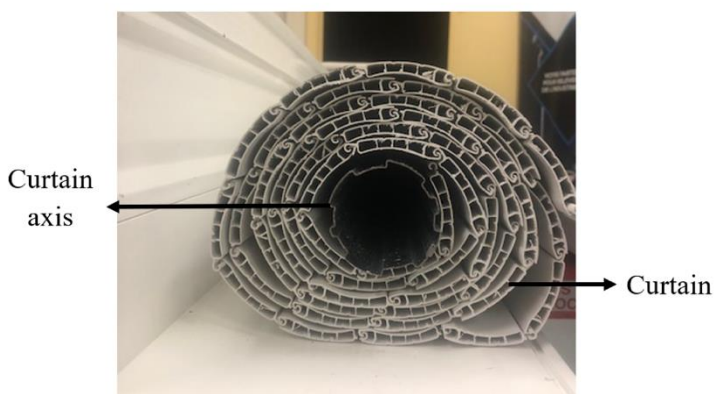

Fig. 4. Configuration of the curtain

The curtain axis (Fig.4) consists of a roller tube, which is a hollow metal tube located within the roller shutter box. The shutter curtain or slats are coiled around the roller tube when the shutter is retracted. A spring or motorized system is used to roll and unroll the shutter for opening and closing. The manual equipment is often less well insulated than its motorized counterparts because of the presence of a strap or crank handle allowing air to pass through.

In addition to being an area of poor thermal and acoustic performance, the casing is also the ideal place for the proliferation of dust, humidity, and other pests. Effective insulation is therefore the obvious solution to deal with these problems and to minimize the impact of external disturbances. Different insulation materials are used such as rock wool, glass wool, expanded polystyrene, melamine foam, and heavy masses. For effective sound insulation against airborne noise, the densest and thickest insulation possible is required. Each area that is not insulated by a few millimeters constitutes a sound bridge that impairs the performance of the box.

3. Experimental measurements of the sound transmission loss

This paragraph provides an overview of the laboratory measurements of sound transmission loss according to ISO 10140 standards [1]. It explains the requirements for the laboratory setup, such as room volume and humidity control. The configuration of the emitting and receiving rooms, including the dimensions, materials, and insulation, are described. The placement of sources and microphones in generating a diffuse sound field and measuring sound pressure levels is given. The paragraph also introduces the concepts of transmission loss and normalized sound insulation index for evaluating the sound insulation performance of building components such as roller shutter boxes.

3.1 Laboratory measurement

To test samples such as windows, air inlets, or roller shutter boxes, there is an opening between the two rooms. When conducting sound loss index measurements in laboratories, the sound transmitted through any indirect path must be negligible compared to the sound transmitted through the sample. For this work, the experimental results are based on the configuration of the emitting and receiving rooms shown in Fig.5. The emission chamber has a volume of 78 m^3, while the receiving chamber has a volume of 62.3 m^3. The receiving room walls are made of concrete with a thickness of 200 mm and separated by a layer of mineral wool for insulation. The wall labeled 3 is made of concrete block with a thickness of 100 mm. The two rooms are placed on spring boxes noted 7. The emitting room has two steel sheets of thickness 2 mm and 6 mm, respectively, separated by mineral wool. The separating wall is noted 6, and the tested box is labeled C.

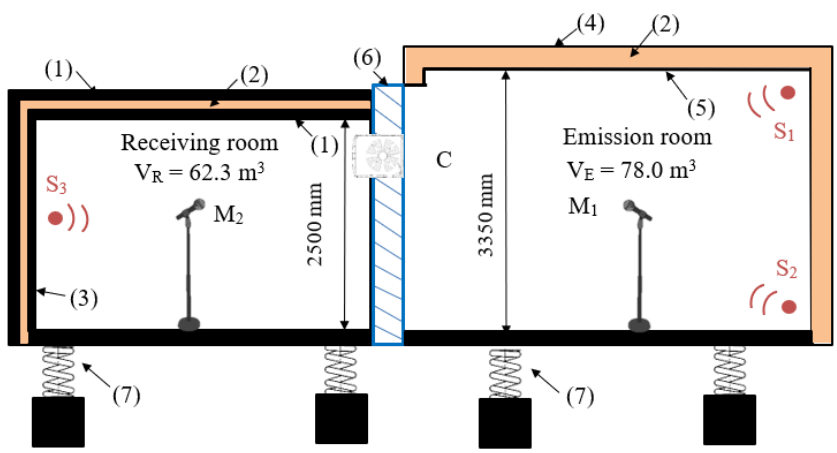

Fig. 5. Experimental set-up of acoustic experimental test

In the emitting chamber, two monopole sources (S_1 and S_2) are placed in the corners of the room to generate several acoustic wave reflections on the walls to create a sufficiently diffuse field. The power incident on the sample is deduced from the sound pressure. A rotating microphone and a sound amplifier in the emitting chamber are used in this room. In the receiving room, there is the presence of a rotating microphone (M_2) and a source (S_3) to measure the reverberation time of the room. The microphone in the receiving room also measures the sound pressure level of the room transmitted by the tested element. Finally, there is the control room where we find a real-time spectrum analyzer allowing us to give the results in the third-octave band, a calibrator, and a computer for the post-processing of results.

Fig. 6. Experimental test of the roller shutter box (a) front view (b) and rear view

The partition wall is constructed using concrete and incorporates a layer of mineral wool. Its conception helps suppress lateral sound transmission. This wall features an opening where a box is positioned (see Fig. 6). The box is then securely mounted on three sides of the wall and screwed at the bottom to a wooden crosspiece sealed with plaster in the test panel. To ensure an airtight seal, the perimeter of the box is sealed using a sealant (depicted in Fig. 7). Two types of boxes were examined: one without any insulating materials, and another enhanced with foam and heavy mass insulation. For each box, the position of the shutter was altered—both rolled-up and unrolled configurations were tested. In total, four experiments were conducted to comprehensively investigate the effects.

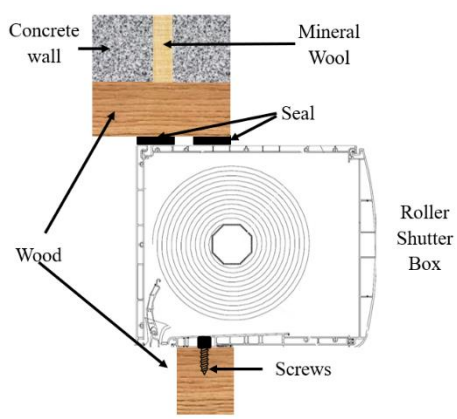

Fig. 7. Cutaway view of shutter box installation during the experiment

3.2 Acoustic indicators

The Sound Reduction Index R (also known as insulation) in dB for the laboratory tests can be derived from the experimental measurements using the following formula [1,15,16,17]:

$$R = L_1 - L_2 + 10\log\left(\frac{S}{A}\right) \tag{1}$$

where L_1 and L_2 are respectively the average sound pressure level in the emission and receiving room, S is the area of the test opening in which the test element is installed in m^2 , and A is the equivalent sound absorption area in the receiving room in m^2 which can be calculated from Sabine formula:

$$T_R = \frac{0.16V}{A} \tag{2}$$

where V is the volume of the receiving room and T_R its reverberation time.

The term $10\log(S/A)$ is designed to bring a correction to the measured values of the transmission loss index, considering both the size of the separating partition and the characteristics of the receiving room. These factors can vary from one laboratory to another. However, the R index is not appropriate for the experimental characterization of roller shutter boxes. The acoustic attributes of these structures are instead represented by the normalized sound insulation index, denoted $D_{n,e}$ or STL (for Sound Transmission Loss) and defined by [1]:

$$D_{n,e} = L_1 - L_2 + 10\log\left(\frac{A_0}{A}\right) \tag{3}$$

where A_0 is a reference equivalent absorption area, taken as 10 m^2.

4. Finite element formulation for structural-acoustic systems with poroelastic materials

The aim of this paragraph is to propose a numerical prediction for the sound transmission of an elastic structure filled with an acoustic fluid and incorporating porous materials. The finite element method is utilized to model the solid, fluid, and porous domains based on the local equations and their variational formulation (not included in this paper for brevity). The excitation of the structure is achieved using a diffuse field, and the sound radiation is computed using either the Rayleigh integral method or the infinite element method, depending on the shape of the structure.

4.1. Local equations

An elastic structure occupying the domain Ω_E and filled with a compressible, non-viscous fluid that occupies a domain Ω_F (Fig. 8) is considered. The effects of gravity are neglected. The structure is clamped on its boundary Γ_u and subject to external forces $\vec{F}^d$ on its boundary Γ_t. The density of the structure is denoted ρ_E, c_A and ρ_A are respectively the speed of sound and the density in Ω_F. The fluid-structure interface is noted $\sum_{EA}$. A poroelastic material of the domain Ω_P is fixed to the elastic structure and in contact with the acoustic domain. The fluid-poroelastic interface is denoted $\sum_{AP}$ and the structure-poroelastic interface is denoted $\sum_{EP}$. $\overrightarrow{n_E}$, $\overrightarrow{n_A}$ and $\overrightarrow{n_P}$ represent the exterior normals of the structure, fluid and poroelastic domains respectively.

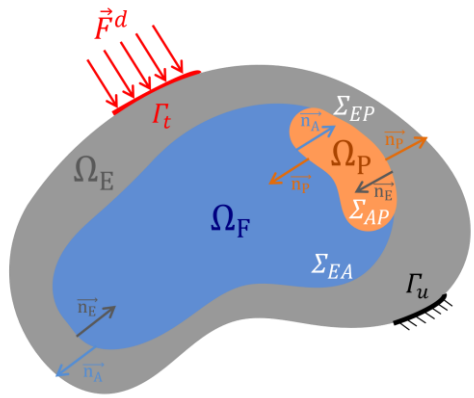

Fig. 8. Coupled fluid-structure-poroelastic problem

The porous material is modeled in this work using Biot theory [8,18]. This theory is applied when the porous material has an elastic matrix. In this case, the material is defined by its porosity ϕ, static flow resistance σ, tortuosity α_∞ , viscous length Λ, and thermal length Λ'. The elastic skeleton is characterized by its Young's modulus E_S, Poisson's ratio ν_S, structural damping coefficient η_S , and its density ρ_S. In total, the poroelastic material is characterized by 9 parameters.

The local equations [8] for the coupled elastic-acoustic-poroelastic problem can be expressed in terms of the following variables: the displacement of the elastic structure $\vec{u}^E$, the displacement of the solid phase of the porous $\vec{u}^s$, the pressure for the fluid phase of the porous p^F and the pressure of the acoustic cavity p^A:

- Elastic structure

$$\text{div}\,\bar{\bar{\sigma}}^E + \rho_E \omega^2 \vec{u}^E = \vec{0}\ ;\ \forall\ M\ \in \Omega_E \tag{4.a}$$

$$\bar{\bar{\sigma}}^E \overrightarrow{n_E} = \overrightarrow{F^d}\ ;\ \forall\ M\ \in \Gamma_t \tag{4.b}$$

$$\vec{u}^E = \vec{0}\ ;\ \forall\ M\ \in \Gamma_u \tag{4.c}$$

- Acoustic cavity

$$\Delta p^A + \frac{\omega^2}{c_A^2} p^A\ =\ 0\ ;\ \forall\ M \in \Omega_F \tag{5}$$

- Poroelastic material (solid phase)

$$\text{div}\,\bar{\bar{\sigma}}^s + \omega^2 \tilde{\rho}_s \vec{u}^S + \tilde{\gamma}\,\vec{\nabla}\,p^F = \vec{0};\ \forall\ M \in \Omega_P \tag{6.a}$$

- Poroelastic material (fluid phase)

$$\frac{\phi^2}{\tilde{\rho}_{22}} \Delta p^F + \omega^2 \frac{\phi^2}{\tilde{R}} p^F - \omega^2 \tilde{\gamma}\,\text{div}\,\vec{u}^S = 0; \forall\ M \in \Omega_P \tag{6.b}$$

where $\bar{\bar{\sigma}}^E$ is the stress tensor of the elastic structure. $\bar{\bar{\sigma}}^s$ is the in vacuo stress tensor of the porous material. It is related to the total stress tensor $\bar{\bar{\sigma}}^t$ of the material through the following relation: $\bar{\bar{\sigma}}^s = \bar{\bar{\sigma}}^t + \phi(1 + \tilde{Q}/\tilde{R})p^F\bar{\bar{1}}$ where $\tilde{Q}$ is an elastic coupling coefficient between the two phases, and $\tilde{R}$ may be interpreted as the bulk modulus of the air occupying a fraction ϕ of a unit volume aggregate. $\tilde{\rho}_{22}$ is the effective density [8]. ω in rad/s is the angular frequency.

Between the acoustic and the elastic structure domains, two coupling conditions must be satisfied [8,19]:

$$\vec{\nabla}p^A.\overrightarrow{n_A} = \omega^2\rho_A\vec{u}^E.\overrightarrow{n_A};\ \forall\ M\ \in \Sigma_{EA} \tag{7.a}$$

$$\bar{\bar{\sigma}}^E\overrightarrow{n_E} = p^A\overrightarrow{n_A};\ \forall\ M\ \in\ \Sigma_{EA} \tag{7.b}$$

Equation (7.a) ensures the continuity of the mean normal displacement while equation (7.b) ensures the continuity of the normal stress at the interface Σ_{EA}.

Between the acoustic and the poroelastic domains, three conditions must be satisfied [19]:

$$p^F = p^A;\ \forall\ M\ \in \Sigma_{AP} \tag{8.a}$$

$$\frac{1}{\rho_A\omega^2}\vec{\nabla}p^A.\overrightarrow{n_P} = \vec{u}^S.\overrightarrow{n_P} + \phi(\vec{u}^F - \vec{u}^S).\overrightarrow{n_P};\ \forall\ M\ \in \Sigma_{AP} \tag{8.b}$$

$$\bar{\bar{\sigma}}^t\overrightarrow{n_P} = p^A\overrightarrow{n_A};\ \forall\ M\ \in \Sigma_{AP} \tag{8.c}$$

where $\vec{u}^F$ is the displacement of the fluid phase of the porous material.

Equation (8.a) represents the continuity of the pressure across the boundary Σ_{AP}. Equation (8.b) ensures the continuity of the relative mass flux. Finally, equation (8.c) represents the continuity of the normal stress.

Between the elastic solid domain and the porous medium, three continuity conditions are present [19]:

$$\vec{u}^S = \vec{u}^E;\ \forall\ M\ \in \Sigma_{EP} \tag{9.a}$$

$$(\vec{u}^F - \vec{u}^S)\overrightarrow{n_P} = 0\ ;\forall\ M \in \Sigma_{EP} \tag{9.b}$$

$$\bar{\bar{\sigma}}^t\overrightarrow{n_P} = -\bar{\bar{\sigma}}^E\overrightarrow{n_E};\ \forall\ M\ \in \Sigma_{EP} \tag{9.c}$$

Equation (9.a) ensures the continuity of displacement between the solid skeleton and the elastic structure. Equation (9.b) expresses the fact that there is no relative mass flux across the boundary Σ_{EP}. Finally, the continuity of the total normal stress between the elastic structure and the poroelastic material is expressed by equation (9.c).

4.2. Finite element discretization

The resolution of the multiphysics problem considered in this work is done with the finite element method. Thus, introducing the vectors of nodal displacements of the elastic structure $\vec{U}^E$ and the solid phase of the porous $\vec{U}^S$ as well as the vectors of nodal pressures in the acoustic cavity $\vec{P}^A$ and in the fluid phase of the poroelastic $\vec{P}^F$, the following coupled matrix system is find from the previous local equations and variational formulation of the problem:

$$\begin{bmatrix} [K_E]-\omega^2[M_E] & -[C_{EA}] & [C_{ES}] & 0 \\ -\omega^2[C_{EA}]^T & [K_A]-\omega^2[M_A] & 0 & [C_{AF}] \\ [C_{ES}]^T & 0 & [K_S(\omega)]-\omega^2[M_S(\omega)] & -[C_{SF}] \\ 0 & [C_{AF}]^T & -\omega^2[C_{SF}]^T & [K_F(\omega)]-\omega^2[M_F(\omega)] \end{bmatrix} \begin{bmatrix} \vec{U}^E \\ \vec{P}^A \\ \vec{U}^S \\ \vec{P}^F \end{bmatrix} = \begin{bmatrix} \vec{F} \\ \vec{0} \\ \vec{0} \\ \vec{0} \end{bmatrix} \quad (10)$$

where $[K_E]$ and $[M_E]$, $[K_A]$ and $[M_A]$, $[K_S]$ and $[M_S]$, $[K_F]$ and $[M_F]$ are the stiffness and mass matrices of the elastic structure, the acoustic cavity, the solid phase and the fluid phase of the porous material respectively. $[C_{EA}]$ and $[C_{SF}]$ are the fluid-structure and poroelastic phases coupling matrices respectively. $[C_{ES}]$and $[C_{AF}]$ are coupling matrices assuring that $\vec{U}^E = \vec{U}^S$ on Σ_{EP} and $\vec{P}^A = \vec{P}^F$ on Σ_{AP} respectively. $\vec{F}$ is the vector of nodal forces applied to the structure.

The system (10) is solved by a direct approach in frequency domain and at each frequency step the frequency-dependent matrices of the porous medium are updated. It leads simultaneously to the nodal displacements of the elastic structure and the porous solid phase and to the nodal pressures in the acoustic cavity and in the fluid porous phase. Note that the $(\vec{u}^S, p^F)$ formulation for the porous material, other than the reduction of the numerical cost, has the advantage of the simplicity of the coupling with other domains compared to the formulation with the displacements of the two solid and fluid phases of the porous. The size of the global system can be also partially reduced by projecting the variables of the elastic structure and the acoustic cavity onto truncated projection bases calculated from the decoupled acoustic fluid-elastic structure modes of the problem. However, due to complex dissipation mechanisms and frequency dependence of the structural and acoustic properties of the porous material, the associated eigenvalue problem is non-linear and prevents the use of reduced projection bases for this domain.

4.3. Diffuse field excitation

To avoid modeling the emitting chamber, the numerical model applies only a diffuse sound field to the structure as an acoustic excitation. A diffuse field refers to a field in which the intensity of sound remains uniform in all directions. It comprises an infinite number of uncorrelated plane waves with random and equal probabilities of incidence. Various methods can be employed to characterize this type of acoustic stimulation [20,21,22]. In the context of this study, the statistical definition of diffuse waves is based on the Power Spectral Density matrix (PSD), represented as $[S_P(\omega)]$. The (i,j) component of this matrix is expressed as follows [23]:

$$[S_P(\omega)]_{(i,j)} = S_{ref}(\omega) f_c\left((P_i, P_j), \omega\right) = S_{ref}(\omega)\frac{\sin kr}{kr} \quad (11)$$

where the spatial correlation function f_c provides a homogeneous diffuse field over the structure, P_i and P_j two points on the charged surface, r the distance between these two points, $S_{ref}(\omega)$ is the reference power spectral density ($S_{ref}(\omega) = 1$ Pa^2/Hz in our case), and k is the acoustic wavenumber.

The Cholesky decomposition efficiently factors the Power Spectral Density matrix $[S_P(\omega)]$ into a lower triangular matrix $[L(\omega)]$ and its complex conjugate transpose, ensuring numerical stability and improved computational efficiency [24]:

$$[S_P(\omega)] = [L(\omega)][L(\omega)]^H \quad (12)$$

where :

$$[L(\omega)]_{(i,i)} = \sqrt{[S_P(\omega)]_{(i,i)} - \sum_{k=1}^{i-1}\left([L(\omega)]_{(k,i)}\right)^2} \tag{13}$$

$$[L(\omega)]_{(i,j)} = \frac{1}{[L(\omega)]_{(i,i)}}\left([S_P(\omega)]_{(i,j)} - \sum_{k=1}^{i-1}[L(\omega)]_{(k,i)}[L(\omega)]_{(k,j)}\right) \text{ when } j > i \tag{14}$$

At each frequency step, the vector of sampled nodal pressures $\vec{P}^S$exerted on the loaded surface defined as follows:

$$\vec{P}^S(\omega) = [L(\omega)]\vec{\varsigma} \tag{15}$$

Where $\vec{\varsigma}$ is the random phase vector defined with the phase angle Φ_n varying from $[0,2\pi]$ for each plane wave, N is the total number of sampled plane waves:

$$\varsigma_n = e^{i\Phi_n}\,; n \in [1,N] \tag{16}$$

Note that the vector $\vec{P}^S$ is utilized as the excitation load on the structure in Equation (10), replacing $\vec{F}$ after being multiplied by the elemental surfaces.

4.4. Estimation of the acoustic radiated power

The Rayleigh integral and the infinite element method (IFEM) are among the various numerical techniques available for calculating the radiated power of a vibrating structure. The selection of either method depends primarily on the structure's geometry and the characteristics of the acoustic radiation domain. Furthermore, these two methods vary in their numerical designs and entail significantly different computational costs. This paragraph provides a concise overview of each method.

The Rayleigh integral offers a method to compute the pressure p at a specific point M within the external acoustic domain, resulting from the vibration of an elastic planar structure radiating into a rigid baffle. This integral equation relies on the knowledge of the normal velocity v_n at any point G on the vibrating plate with surface Γ. The Rayleigh integral is frequency dependent and can be expressed as follows [25,26,27]:

$$p(\omega, M) = \rho_0 \frac{i\omega}{2\pi}\int_\Gamma v_n(\omega, G)\frac{e^{-ikr}}{r}dS \tag{17}$$

where ρ_0 is the volume density of the external acoustic domain, k is the wave number ($k = \omega/c_0$), c_0 is the speed of sound in the acoustic domain and r is the distance between M and G. The velocity distribution $v_n(\omega, G)$ can be obtained through finite element simulation. Therefore, the radiated power is given by:

$$W_r = \frac{1}{2}\,\mathrm{Re}\left(\int_\Gamma p(G)v_n^*(G)dS\right) \tag{18}$$

where v_n^* is the complex conjugate of the normal velocity and Re is the real part of the expression. After partitioning the vibrating baffle panel into rectangular elements [26], the last integral equation is transformed into a matrix equation. This matrix equation relates the surface velocities of the individual elements to the sound power radiated in different directions or at different observation points.

The Infinite Element Method (IFEM) is a numerical technique employed for solving problems that require compliance with the Sommerfeld condition, preventing the return of acoustic waves and facilitating the dispersion of pressure waves in the far field. By coupling finite elements within the truncated domain with infinite elements on the boundaries, the IFEM ensures the proper transmission of energy radiated by a vibrating structure into the surrounding region. This method enables an accurate estimation of the radiated sound power. To mitigate sound wave reflections at the boundary of the truncated acoustic domain, the IFEM incorporates special shape functions, denoted as Ψ. These shape functions can be described as follows [28,29]:

$$\Psi(r,\theta,\varphi) = e^{-jkr} \sum_{n=1}^{m} \frac{F_n(\theta,\varphi)}{r^n} \tag{19}$$

where (r,θ,φ) are the ellipsoidal reference coordinate, m is the radial interpolation order and $F_n(\theta,\varphi)$ is a continuous regular function in the infinite fluid domain [23,28]. For this work, the interpolation order m is 10.

The Rayleigh integral is a computationally efficient method, as it requires less calculation time. However, its applicability is limited to plane baffled structures that radiate in either an unbounded acoustic domain or a bounded acoustic domain with absorbent walls. On the other hand, the infinite element method, despite being more computationally expensive compared to the Rayleigh integral, offers the advantage of being applicable to structures of any geometric shape, including non-plane structures, radiating in either a bounded acoustic domain or an unbounded one.

In this research, we studied boxes with a slightly domed radiating surface within the frequency range of 100 to 1000 Hz. To ensure a comprehensive and accurate assessment in line with our experimental measurements, we have chosen to employ the infinite elements method within the frequency range of interest. This choice guarantees the precision required for a comparison against our obtained results.

5. Sound transmission through roller shutter box

5.1. Characterization of the investigated roller shutter box and its numerical model

The studied box (Fig.9.a) is made of PVC (PolyVinyl Chloride) with the following mechanical properties: E_b = 2.8 GPa, ν_b = 0.35, ρ_b = 1460 kg/m^3 and η_b = 0.04. Its dimensions are: 210 mm x 250 mm x 1450 mm. The end caps of the box, with 10 mm thick, are made of ABS (Acrylonitrile Butadiene Styrene) which is an industrial thermoplastic polymer with the following mechanical properties: E_c = 2.9 GPa, ν_c = 0.42 ρ_c = 1100 kg/m^3 and damping coefficient η_c = 0.01. Material properties are provided by the manufacturers.

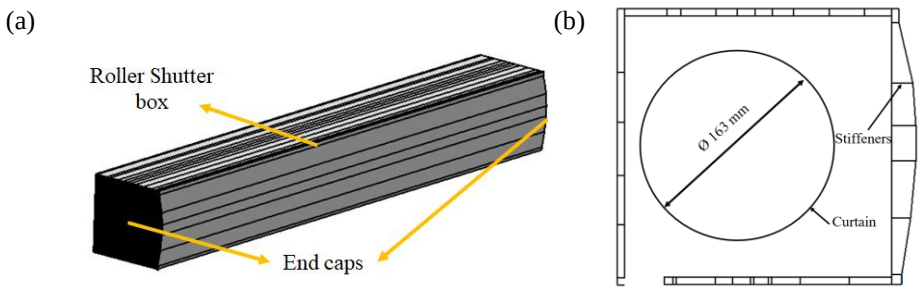

Fig.9. The CAD model of (a) the complete roller shutter box and (b) the profile of the roller shutter box retracted.

The box structure consists of double-leaf panels with stiffeners, where each wall and stiffener have a thickness of 1.5 mm, as illustrated in Fig.9.b. The boundary conditions employed in the laboratory tests include screwing the box onto surface 2 (as depicted in Fig. 10.a) and ensuring an airtight seal with a sealant joint on surfaces 1, 1', and at the edges of surface 3, as shown in Fig. 10.b. Finally, we consider that the roller shutter box is filled with air (c = 340 m/s, ρ = 1.225 kg/m^3 and η = 0.01). The curtain's structure has been intentionally omitted from the model to achieve simplicity. Instead, the air cavity inside the box is represented with a holed circle, serving as a marker for the curtain's position. Depending on whether the curtain is retracted or extended, the diameter of this cavity hole varies (retracted: 163 mm, extended: 60 mm). As the curtain and its axis are considered as rigid solid cylinders, sound waves transmission through their volume is prevented, eliminating the need to mesh the circle for both configurations.

To reduce the sound transmission through the roller shutter box, a porous material (melamine foam) in combination with heavy viscoelastic masses are introduced in the system (Fig.10.b). The mechanism of melamine foam revolves around its ability to absorb sound energy using its open-cell structure. In addition, the heavy mass consists of viscoelastic materials employed for vibration damping and providing additional mass. Bitumen, a commonly utilized material in construction and industrial applications, is extensively employed in heavy masses. When exposed to mechanical vibrations, the insulation materials absorb a portion of the vibratory energy by converting it into heat. To maintain simplicity, this work adopts a linear, homogeneous, and viscoelastic heavy mass. In the isotropic case, the viscoelastic material is characterized by a Poisson's ratio ν real and frequency independent and a complex Young's modulus E^* expressed in the following form:

$$E^* = E(1 + i\eta) \tag{20}$$

The used melamine is characterized by the following parameters: E_f = 120 kPa, ν_f = 0.1, ρ_f = 750 kg/m^3, η_f = 0.15, σ = 10000 N.m^{-4}.s, ϕ = 0.98, α = 1, Λ = 0.0001 m and Λ' = 0.0003 m. It's modeled using Biot theory [30,31]. The heavy mass, of 4 mm thickness, has the following properties: E_h = 120 MPa, ν_h = 0.43, ρ_h= 1600 kg/m^3 and η_h = 0.65. Note that we compared the Biot theory with the equivalent fluid model and found that the Biot model yielded better results, especially at lower frequencies. This justified our preference for the Biot model as it effectively considers interactions between the solid and fluid phases in porous materials.

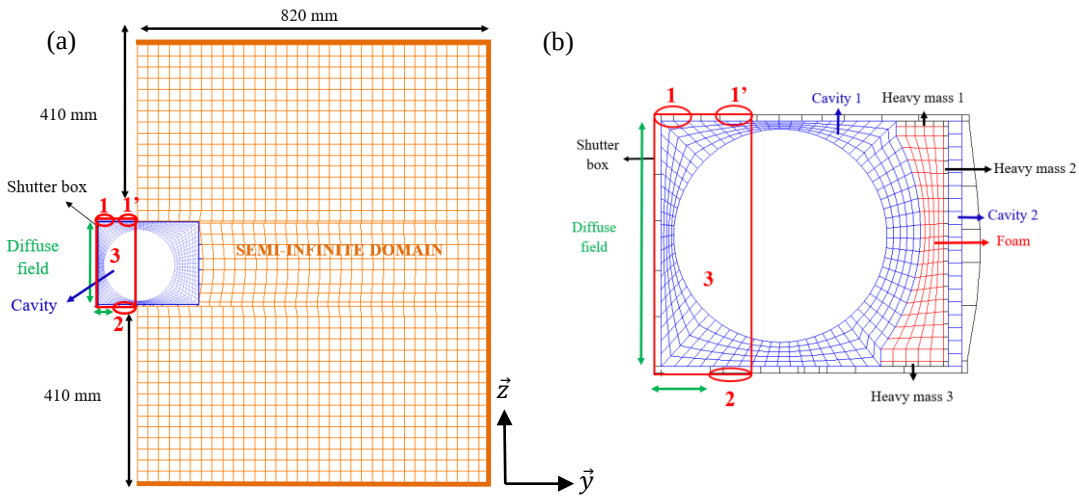

Fig.10. Numerical model used for acoustic simulation of the retracted roller shutter box: (a) Non-isolated configuration and (b) Isolated configuration with melamine foam and heavy masses

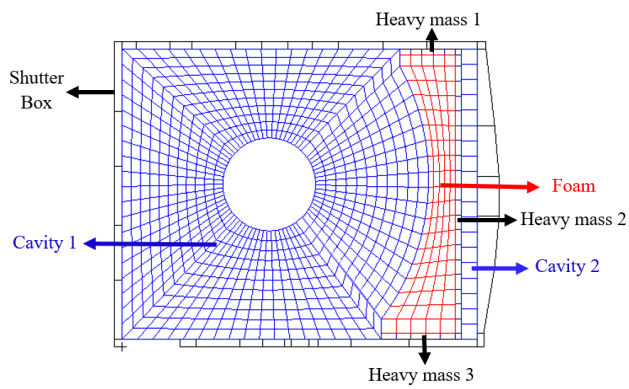

Fig.11. Numerical model used for acoustic simulation of the extended and isolated roller shutter box with melamine foam and heavy masses

Concerning the numerical model, the panels and stiffeners of the box were meshed with linear quadrilateral elements of size 10 mm. Figs.10 and 11 show a cross-section of the 3D numerical model. The emission room is replaced by a diffuse field. The proposed Cholesky method is applied for the treatment of the diffuse field with maximal normal angle of 90 degrees and 30 realizations [3,29]. The receiving chamber is replaced by a parallelepiped-shaped domain of dimensions 820 mm x 1030 mm x 1850 mm meshed with hexahedral elements of size 25 mm and filled with air (c_{IE} = 340 m/s and ρ_{IE} = 1.225 kg/m3 and η_{IE} = 0.02). The dimensions of the semi-infinite domain were found by a convergence study, changing one dimension at a time to find a stable result. To prevent acoustic wave reflections, 2D quadrilateral infinite elements of size 25 mm are applied at the border of this domain (Fig.8.a). The damping coefficients within the acoustic domains were fine-tuned via a convergence study that compared simulation results with experimental tests. However, to

maintain brevity, the specifics of this comparison are not expounded upon in this paper. The transmitted power is calculated with Actran software. The foam and heavy masses were also meshed with hexahedral elements respectively of size 9 mm and 4 mm. The cavities numbered 1 and 2 of the roller shutter box were mesh with hexahedral element of size 10 mm. Fig. 11 shows the numerical model of the roller shutter box in extended position.

5.2. Correlation between numerical and experimental results

In this section, we examine and analyze the correlation between numerical predictions and laboratory results regarding sound transmission through the roller shutter box. The study will also investigate the impact of introducing melamine foam and heavy mass acoustic treatment, as depicted in Fig.10.b.

To evaluate the effectiveness of the soundproofing treatments, Fig. 12 and Fig.13 illustrate a comparison of the sound transmission loss (measured in dB) obtained from laboratory experiments and calculated numerically in third octave bands for the curtain retracted and extended respectively. The gap in Fig. 12 and Fig. 13 corresponds to the absolute difference between the experimental and numerical values. In Fig.12.a and Fig.13.a, we present the results obtained without soundproofing's treatment and in Fig.12.b and Fig.13.b with treatment. Additionally, Table 1 presents the numerical results for the effect of melamine and heavy mass within the frequency range of interest.

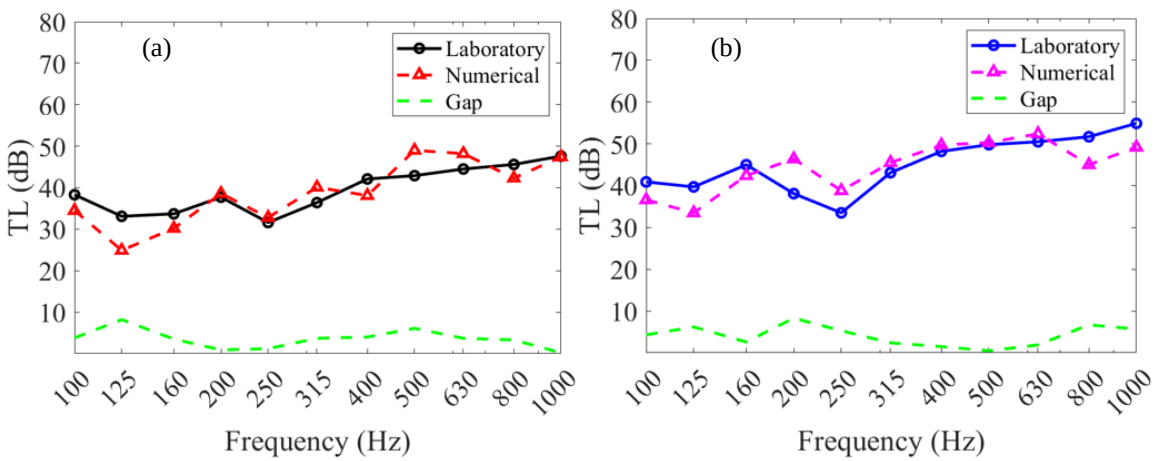

Fig.12. Comparison of Sound Transmission Loss between numerical and experimental results for retracted Roller Shutter Box: (a) Non-isolated configuration (b) Isolated configuration with melamine foam and heavy masses

For all the cases studied, the average absolute difference between the experimental results and the numerical calculations remains below 10%. This indicates the validation of our numerical model for predicting the sound transmission of roller shutter boxes. This model will be utilized in the subsequent part of the next section to optimize the structure and conduct further investigations. Finally, we compared the outcomes obtained using the proposed Infinite Element Method with those from the Rayleigh Integral Method. To apply the Rayleigh Integral Method, we simplified the shape of the roller shutter box's "trap door" from its curved form to a flat shape radiating into a semi-infinite space. This simplification excluded radiation from nearby surfaces perpendicular to the "trap door". The comparison revealed a significant deviation in the

results produced by the Rayleigh Integral Method. This discrepancy highlights the Rayleigh integral approach's inability to effectively investigate the acoustic properties of our roller shutter box."

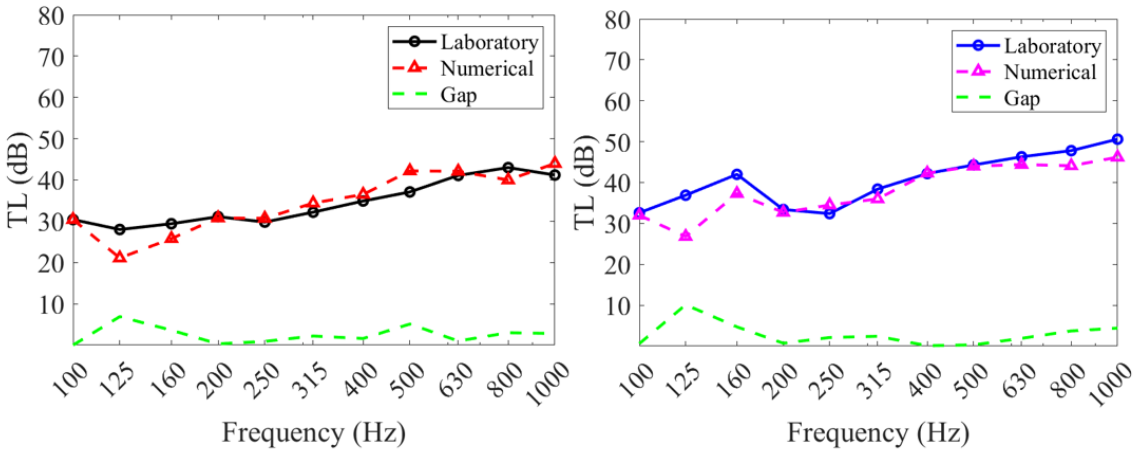

(a) (b)

Fig.13. Comparison of Sound Transmission Loss between numerical and experimental results for extended Roller Shutter Box: (a) Non-isolated configuration (b) Isolated configuration with melamine foam and heavy masses

Tables 1 clearly demonstrates the positive impact of introducing insulating materials on the acoustic performance of the roller shutter box, regardless of the position of the curtain. The numerical results indicate an average gain of 5.4 dB when the curtain is retracted and 4.0 dB when the curtain is extended. These findings suggest that the combination of a retracted curtain and insulation materials offers the most effective acoustic performance.

Table 1 – Sound Transmission Loss (dB) comparison for numerical analysis of retracted and extended roller shutter boxes:(a) Non-isolated, (b) Isolated: melamine foam and heavy masses

Frequency (Hz)	**100**	**125**	**160**	**200**	**250**	**315**	**400**	**500**	**630**	**800**	**1000**
Retracted											
(a)	34,5	24,9	30,2	38,6	32,8	40,1	38,1	49,0	48,2	42,3	47,4
(b)	36,6	33,5	42,4	46,4	38,8	45,5	49,7	52,3	52,4	45,0	49,2
Extended											
(a)	30,4	21,1	25,8	30,8	30,7	34,4	36,5	42,2	42,1	40,0	44,0
(b)	32,0	26,8	37,3	32,7	34,5	36,0	42,3	44,0	44,4	44,1	46,2

Given that the curtain and its axis are treated as solid, rigid cylinders, sound wave transmission through the curtain's volume is effectively prevented. When the curtain is retracted, its volume increases compared to its unrolled state. This expansion is responsible for the observed reduction in sound transmission during retraction.

6. Parametric analysis

6.1. Influence of end caps

The end caps of a roller shutter box serve multiple important functions and play a vital role in its overall performance. Firstly, end caps act as a protective barrier, safeguarding the contents of the box from potential damage and external environmental factors. They effectively prevent dust, dirt, and debris from entering the box, ensuring the integrity and cleanliness of the enclosed space. In addition to their protective role, end caps are designed to aesthetically match the appearance and finish of the rest of the roller shutter.

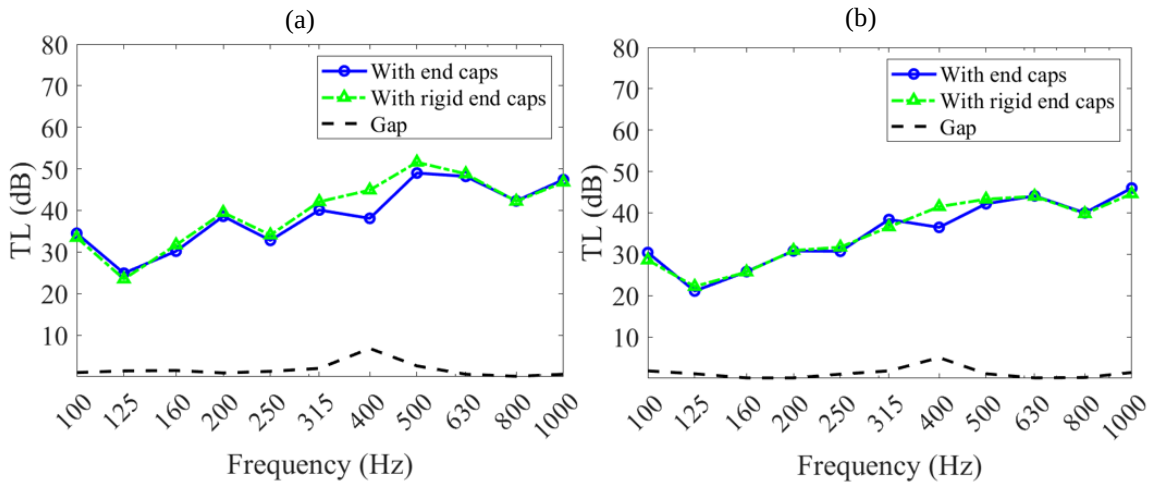

Fig. 14. Impact of end caps on numerically computed Sound Transmission Loss (dB) for Non-isolated roller shutter boxes: (a) retracted and (b) extended

We conducted an investigation to explore the impact of end caps on the sound transmission characteristics of the roller shutter box without insulation. Specifically, we examined two scenarios: one with elastic end caps and another with rigid end caps (where the side surfaces of the box were treated as rigid end caps). We evaluated the sound transmission loss for both the retracted curtain (Fig. 14.a) and the extended curtain (Fig. 14.b) in third band octave.

Interestingly, our findings indicate that the effect of end caps does not significantly affect the sound transmission loss in either position of the curtain. In other words, the end caps do not appear to have a noticeable influence on the reduction of sound transmission. It is important to highlight that significant enhancements are evident when incorporating rigid end caps specifically at a frequency of 400 Hz. Our observations reveal a remarkable increase of 6.8 dB in acoustic performance when the curtain is retracted, and a substantial gain of 5 dB when the curtain is extended, both occurring at 400 Hz. This suggests that the rigid end caps may contribute to a slight enhancement in sound transmission loss at this specific frequency.

6.2. Influence of the boundary conditions of the box

Boundary conditions refer to the constraints and characteristics imposed on the system's boundaries or interfaces. These conditions can include factors such as type of installation, sealing mechanisms, and connection details. For example, incorporating sealing mechanisms at the interfaces of the roller shutter box can enhance its acoustic performance by reducing air leakage and preventing sound waves from bypassing the enclosure. In this section, the influence of the boundary conditions of the box on the sound transmission loss in the absence of insulation materials is investigated. Both positions of the curtain are studied. Four configurations are considered. The first configuration represents the boundary conditions of the box during the laboratory tests. The box is screwed in surface 2 and on surfaces 1 and 1' a silicone sealant is applied to ensure airtightness. Surface 3 corresponds to the part of the end caps in contact with the wooden test panel. A seal joint is applied at the boundaries of this surface (Fig.10.b). The three translations along x, y and z were blocked for the screwed part and only the translation along x for the part with the seal. In configuration 2, we have blocked the translation along x and along z for the part with the sealant leaving the screwed part unchanged. In configuration 3, we have blocked the three translations for the screwed part and for the part with the seal. Finally, the box is clamped (blocking of the 3 translations and 3 rotations) for configuration 4.

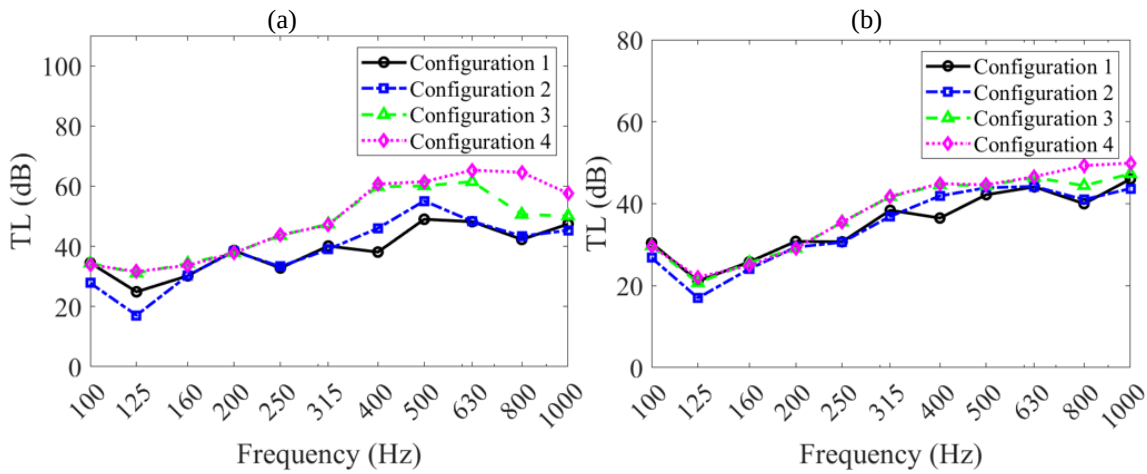

Fig.15. Impact of boundary conditions on numerically computed Sound Transmission Loss (dB) for Non-isolated roller shutter boxes:

(a) retracted and (b) extended

It is evident that the incorporation of boundary conditions plays a crucial role in enhancing the stiffness and overall performance of the structure. When comparing the retracted (Fig.15.a) and extended (Fig.15.b) cases, the impact of boundary conditions becomes apparent, although there is relatively little variation between configuration 1 and configuration 2. However, when examining configuration 3 and 4, significant improvements in sound transmission loss can be observed, particularly in the case where the curtain is retracted. This implies that the arrangement of boundary conditions, in combination with the retracted curtain, contributes to a more effective reduction of sound transmission within the box.

Among the various configurations, configuration 4 stands out as particularly promising in terms of acoustic performance. In fact, a clamped boundary condition, the structure is rigidly fixed at the boundaries, which

restricts its ability to vibrate and transmit sound energy compared to other conditions. The implementation of this configuration results in the most favorable outcomes for sound transmission loss in the box, suggesting that it offers the best potential for minimizing noise propagation and enhancing acoustic insulation.

6.3. Influence of the position of the sound insulation material

Sound insulation materials are specifically engineered to minimize the transmission of sound by effectively absorbing sound waves. In the context of a roller shutter box, the placement of these materials plays a significant role in determining the level of sound transmission loss. It is crucial to consider the positioning of the insulation materials relative to the trapdoor.

To illustrate this point, two configurations are compared. The first configuration, as depicted in Fig.10.b and Fig.11, involves the foam and heavy mass being unbonded and not attached to the trapdoor. The second configuration, shown in Fig.17.a, involves bonding the foam and heavy mass directly onto the trapdoor. By examining these two setups, the impact of the insulation materials' placement can be assessed in terms of sound transmission loss.

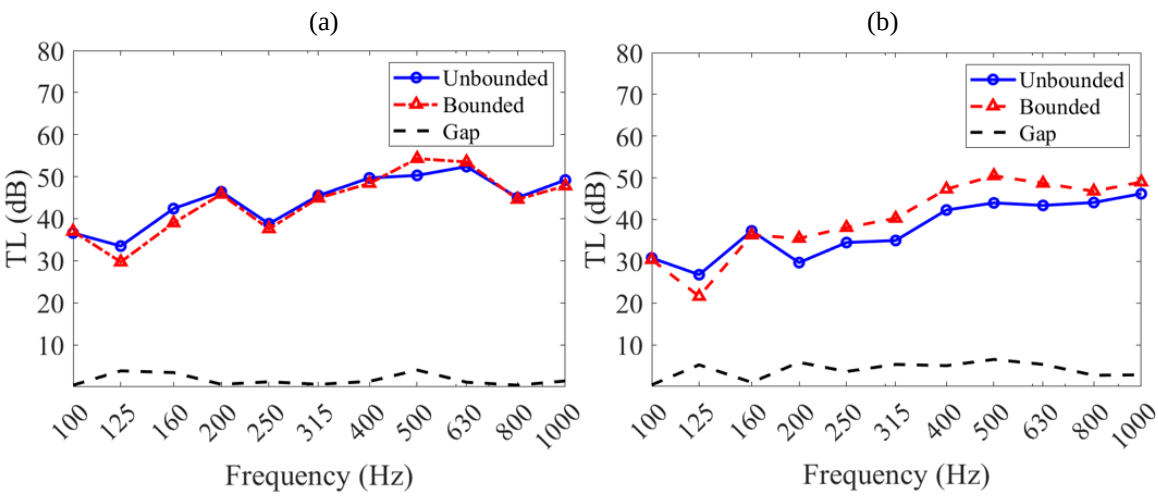

Fig. 16. Impact of position of the sound insulation material (melamine foam and heavy masses) on numerically computed Sound Transmission Loss (dB) for Isolated roller shutter boxes: (a) retracted and (b) extended

The position of the retracted curtain does not show significant differences between the unbonded and bonded cases (Fig. 16.a). The retracted curtain acts as a barrier that prevents the easy passage of vibrations and noises contributing to the overall sound insulation performance. Its presence alone plays a vital role in reducing sound transmission, regardless of the position of the insulation material.

Within the frequency range of 100 Hz to 200 Hz., when the insulation materials are bonded to the trapdoor in both the retracted and extended curtain configurations, a slight deterioration in sound transmission performance is observed. This phenomenon can be attributed to the absence of an air cavity between the insulation material and the trapdoor. The air cavity typically serves as an additional layer of sound insulation

by providing an acoustic insulator. Without it, there is a minor influence on sound transmission within this specific frequency range, resulting in a slightly decreased sound transmission loss.

Conversely, beyond 200 Hz, the extended curtain configuration demonstrates an improvement in sound transmission loss (Fig. 16.b). This suggests that the combination of the extended curtain and the bonded insulation materials enhances the box's ability to attenuate sound, particularly at higher frequencies. Our analysis demonstrates an average gain of 4.6 dB from 200 Hz. Overall, while the position of the insulation material has minimal impact on the retracted curtain configuration, it becomes more relevant when the curtain is extended.

6.4. Optimization of the placement of heavy masses

The incorporation of heavy masses strategically can improve the overall soundproofing performance of the box since they are known for their density and mass, which effectively block sound waves and reduce sound transmission. Optimizing the number of heavy masses depends on various factors, such as the design, dimensions, materials used, and desired level of sound insulation for the roller shutter box. Increasing the number of heavy masses can potentially enhance soundproofing by providing additional barriers to sound transmission. However, there may be diminishing returns when adding multiple heavy masses. Beyond a certain point, the benefits of adding more heavy masses may become less significant or even negligible. In this section, our focus is on optimizing the placement of heavy masses within the box to maximize sound insulation. We examine three different configurations to study their impact on soundproofing. Configuration 1 corresponds to the setup where the insulation materials are bonded to the trapdoor, as depicted in Fig.17.a. This configuration serves as our baseline. Building upon Configuration 1, Configuration 2 involves the addition of a heavy mass on the inner underside of the box, as shown in Fig.17.b. Expanding upon Configuration 2, Configuration 3 replicates Configuration 2 while introducing an additional heavy mass on the upper inner side of the box, as illustrated in Fig.17.c. The added heavy thicknesses are 4 mm.

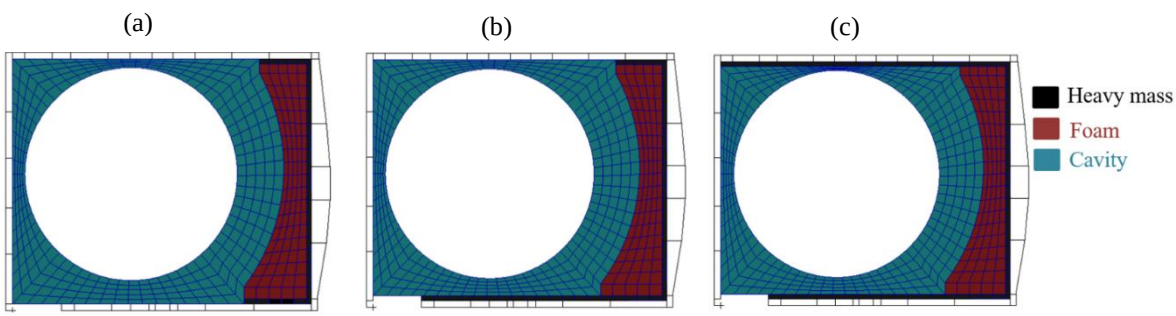

Fig. 17. (a) Configuration 1, (b) Configuration 2 and (c) Configuration 3

Configuration 2 shows a slight improvement in sound insulation compared to Configuration 1 with an average gain of 2.3 dB. This indicates that the inclusion of a heavy mass on the inner underside of the box contributes to a modest enhancement in reducing sound transmission, even with the curtain in a retracted position (Fig.18.a). It is important to note that the retracted curtain itself acts as an effective insulator, plays a critical role in sound transmission reduction within the box.

In the comparison between Configuration 1 and Configuration 3 for the curtain retracted, there are no significant improvements observed in terms of sound insulation (Fig.18.a). During our investigation, we have identified an average gain of 1.3 dB within the frequency range of 100 Hz to 315 Hz. However, beyond 315 Hz, the acoustic performance of the box begins to decline. This suggests that the addition of an extra heavy mass on the upper inner side of the box, as implemented in Configuration 3, does not significantly enhance soundproofing when the curtain is retracted.

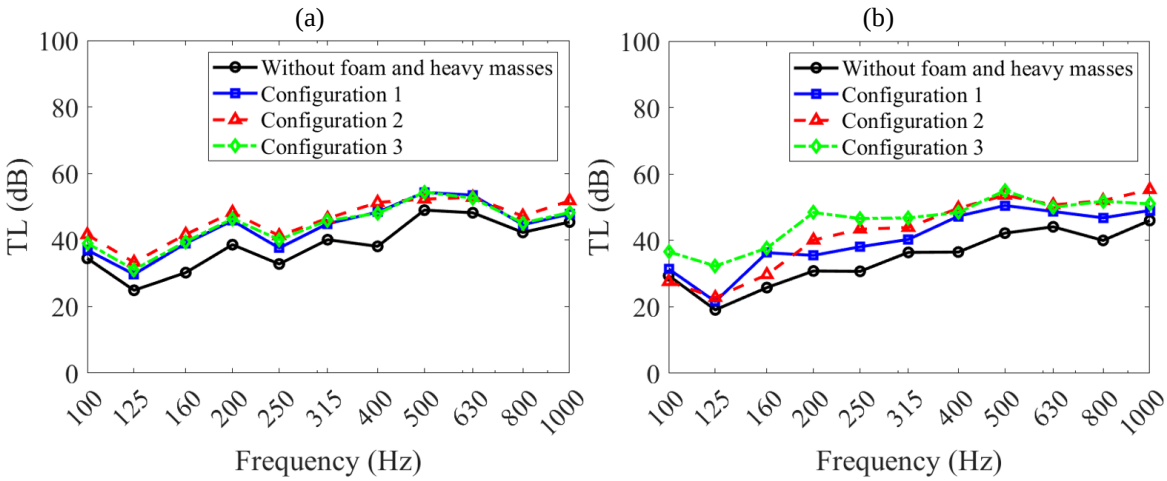

Fig. 18. Impact of position and number of heavy masses on numerically computed Sound Transmission Loss (dB) for roller shutter boxes: (a) retracted and (b) extended.

In the case of the extended curtain, Configuration 2 demonstrates a significant improvement in the performance of the box, particularly from 200 Hz onwards with an average gain of 4.1 dB. This indicates that the addition of a heavy mass on the inner underside of the box effectively enhances sound transmission loss. However, there is a noticeable decline in the acoustic performance of the box between 100 Hz and 160 Hz (Fig.18.b).

Furthermore, Configuration 3 also showcases an improvement in sound transmission loss, specifically within the frequency range of 100 Hz to 315 Hz (Fig.18.b). Based on the analysis conducted, we can deduce an average gain of 5.5 dB. This suggests that the inclusion of an extra heavy mass on the upper inner side of the box, as seen in Configuration 3, further enhances soundproofing within the frequency range of interest.

However, beyond 315 Hz, the results of Configuration 2 and Configuration 3 are indistinguishable in Fig.18.b. This implies that the benefits gained from adding a heavy mass on the upper face of the inner side of the box become less relevant in terms of sound transmission loss beyond this frequency. These findings emphasize the importance of carefully considering the placement and number of heavy masses to optimize sound insulation performance in the extended curtain configuration.

7. Conclusions

In this research, we have successfully developed a numerical model to characterize the acoustic properties of roller shutter boxes in various scenarios, considering insulated and non-insulated conditions as well as retracted and extended curtain positions. Our approach involved utilizing a combination of finite and infinite element methods. Through laboratory experiments and numerical simulations, we obtained results that exhibited a high level of agreement, validating the accuracy of our model. In our model, the incorporation of a free field for the emission room and the use of IFEM for the receiving room guarantees complete uniformity in the acoustic field, even at extremely low frequencies. This approach also prevents the emergence of modal behavior within the two enclosed spaces. As a result, concerns regarding reproducibility are mitigated, as this setup exclusively assesses the inherent capabilities of the element under examination.

Following the validation of our numerical model, we conducted a parametric study to further explore the factors influencing sound transmission in roller shutter boxes. First, we investigated the influence of modeling the end caps. We found that whether we employed elastic properties or simplified the approach with rigid end caps, the effect on sound transmission loss within the box was not substantial. This trend held across most frequencies, except for a distinct enhancement at 400 Hz.

Next, a comparative analysis of sound insulation in both retracted and extended states underscored the pivotal role of boundary conditions. While differences between the original laboratory test configuration (screwed and sealed) and the partially constrained setup (sealed section with limited translations) are relatively minor, configurations featuring a fully clamped arrangement demonstrate significant improvements in sound transmission loss, particularly when the curtain is retracted.

We also studied the role of sound insulation materials in reducing sound transmission within roller shutter boxes. The positioning of these materials relative to the trapdoor was found to be crucial in determining the level of sound transmission loss. While the retracted curtain itself acts as a barrier, reducing vibrations and contributing to sound insulation, bonding insulation materials to the trapdoor led to a slight deterioration in sound transmission performance within the frequency range of 100 Hz to 200 Hz, due to the absence of an air cavity. However, in the extended curtain configuration, our analysis demonstrated an improvement in sound transmission loss with an average gain of 4.6 dB from 200 Hz.

Furthermore, we investigated the optimization of sound insulation by strategically placing heavy masses. Configuration 2, with a heavy mass on the inner underside, showed a slight improvement in sound insulation compared to configuration 1 when the curtain was retracted. Configuration 3, with an additional heavy mass on the upper inner side, did not significantly enhance soundproofing in the retracted curtain configuration, as the curtain itself played a crucial role in reducing sound transmission. However, for the extended curtain configuration, Configuration 2 demonstrates a significant improvement in sound transmission loss from 200 Hz onwards. Configuration 3 also improves sound transmission loss within the range of 100 Hz to 315 Hz. However, beyond 315 Hz, the benefits of adding a heavy mass on the upper inner side become less relevant.

The prospects of this work involve improving the optimization of the acoustic insulation performance of the roller shutter box. This will be achieved by identifying the geometric, mechanical, and acoustic parameters of the materials used that have the most significant impact on sound transmission. To reduce the costs associated with numerical simulations, a global sensitivity analysis will be conducted using a metamodel. Furthermore, structure-borne sound transmission and alternative forms of excitations will be explored in order to optimize the form and position of the porous and heavy-mass materials.

Acknowledgements

The authors would like to express gratitude to CODIFAB (Comité professionnel de Développement des Industries Française de l'Ameublement et du Bois) and UFME (Union des Fabricants de Menuiseries) for their cooperation.

References

[1] ISO 10140: Acoustics - Laboratory measurement of sound insulation of building components, 2021.
[2] Nélisse H, Nicolas J. Characterization of a diffuse field in a reverberant room. *J Acoust Soc Am*. 1997;101(6):3517–24.
[3] Soussi C, Aucejo M, Larbi W, Deü J-F. Numerical analyses of the sound transmission at low frequencies of a calibrated domestic wooden window. *Proceedings of the Institution of Mechanical Engineers, Part C: Journal of Mechanical Engineering Science*. 2021;235(14):2637-2650.
[4] Yang Y, Mace BR., Kingan, MJ. Prediction of sound transmission through, and radiation from, panels using a wave and finite element method. *J. Acoust. Soc. Am.* 2017; 141(4): 2452–2460.
[5] Yang Y, Mace BR., Kingan, MJ. Vibroacoustic analysis of periodic structures using a wave and finite element method. *Journal of Sound and Vibration.* 2019; 457: 333–353.
[6] Ungar EE. Statistical energy analysis of vibrating systems. *Journal of Engineering for Industry*. 1967;89(4):626-632.
[7] Lyon RH. Statistical energy analysis of dynamical systems, theory and application. MIT Press. 1975.
[8] Allard JF, Atalla N. Propagation of Sound in Porous Media: Modelling Sound Absorbing Materials. 2nd Edition. John Wiley & Sons. 2009.
[9] Arne Dijckmans, Gerrit Vermeir, Numerical Investigation of the Repeatability and Reproducibility of Laboratory Sound Insulation Measurements, Acta Acustica united with Acustica 99(3):421-432, 2013.
[10] Ruiqian Wang, Dan Yao, Jie Zhang, Xinbiao Xiao,Ye Li; Effect of installation conditions on laboratory sound insulation measurement and an equivalent method for simply supported boundary, Applied Acoustics 188, 108593, (2022)
[11] ISO 12999-1: Determination and application of measurement uncertainties in building acoustics — Part 1: Sound insulation, 2020.
[12] Asdrubali F, Buratti C. Sound intensity investigation of the acoustics performances of high insulation ventilating windows integrated with rolling shutter boxes. *Appl. Acoust.* 2005;66(9): 1088-1101.
[13] Díaz C, Pedrero A. An experimental study on the effect of rolling shutters and shutter boxes on the airborne sound insulation of windows. *Appl. Acoust.*2009;70(2): 369-377.
[15] Soussi C, Aucejo M, Larbi W, Deü J-F. Numerical analyses of the sound transmission at low frequencies of a calibrated Insulating Glazing Unit. *Appl. Acoust.*2021;179: 108065.
[16] Guyader JL, Lesueur C. Acoustic transmission through orthotropic multilayered plates, part II: Transmission loss. *Journal of Sound and Vibration*.1978;58(1): 69–86.
[17] Soussi C, Aucejo M, Larbi W, Deü JF. Sound transmission through double-glazed window: Numerical and experimental analyses. In *Proceedings of ICA 2019*, Aachen, Germany.
[18] Vigran TE. Building acoustics. Taylor & Francis. 2008.
[19] Sgard FC, Atalla N, Nicolas J. A numerical model for the low frequency diffuse field sound transmission loss of double-wall sound barriers with elastic porous linings. *J. Acoust. Soc. Am.*2000;108(6): 2865-2872.
[20] Atalla N, Panneton R, Debergue O. A mixed displacement-pressure formulation for poroelastic materials. *The Journal of the Acoustical Society of America*.1998;104(4):1444- 1452.
[21] Van den Nieuwenhof B, Lielens G, Coyette JP. Modeling acoustic diffuse fields: updated sampling procedure and spatial correlation function eliminating grazing incidences. In *Proceedings of ISMA 2010*. Leuven, Belgium.
[22] Pierce AD, Beyer RT. Acoustics: An Introduction to its Physical Principles and Applications. 3rd Edition. Acoustical Society of America. 1989.
[23] Vér IL, Beranek LL. Noise and Vibration Control Engineering. Principles and Applications. 2nd Edition. Wiley. 2006.
[24] Free Field Technologies. Actran 22.1 User's Guide Volume 1 Installation, Operations, Theory and Utilities. p.432-433. 2022.
[25] Watkins D. Fundamentals of Matrix Computations. p.36. John Wiley & Sons, Inc. 1991.

[26]Fahy F, Gardonio P. Sound and Structural Vibration. 2nd Edition. Academic Press. 2006.
[27]Larbi W, Deü J-F, Ohayon R. Finite element reduced order model for noise and vibration reduction of double sandwich panels using shunted piezoelectric patches. *Appl. Acoust.*2016;108: 40-49.
[28]Larbi W, Deü J-F, Ohayon R. Vibroacoustic analysis of double-wall sandwich panels with viscoelastic core. *Computers & Structures*.2016;174: 92-103.
[29]Coyette JP, Van den Nieuwenhof B. A conjugated infinite element method for half-space acoustic problems. *J. Acoust. Soc. Am.*2000;108(4):1464-1473.
[30]Lloret MG. Prediction of the airborne sound transmission through a car front end model including poroelastic acousitc treatments. PhD Dissertation, Magdeburg University.2018.
[30]Panneton R, Atalla N. Numerical prediction of sound transmission through finite multilayer systems with poroelastic materials. *The Journal of the Acoustical Society of America*.1996;100(1): 346–354.
[31]Atalla N, Hamdi MA, Panneton R. Enhanced weak integral formulation for the mixed (u, p) poroelastic equations. *The Journal of the Acoustical Society of America.*2001;109(6): 3065–3068.